metals

MDPI

Article

Structure and Properties of Metal-Matrix Composites Based on an Inconel 625–TiB_2 System Fabricated by Additive Manufacturing

Vladimir Promakhov *, Alexey Matveev, Olga Klimova-Korsmik, Nikita Schulz, Vladislav Bakhmat, Artem Babaev and Alexander Vorozhtsov

Center for Additive Technologies, National Research Tomsk State University, Lenin Avenue, 36, 634050 Tomsk, Russia; alekey.9595@mail.ru (A.M.); o.klimova@ltc.ru (O.K.-K.); schulznikita97@gmail.com (N.S.); bakhmatvr@gmail.com (V.B.); temkams@mail.ru (A.B.); abv1953@mail.ru (A.V.)

* Correspondence: vvpromakhov@mail.ru

Abstract: This research work studies the structural phase parameters and physicomechanical properties of metal-matrix composite materials based on a Ni–TiB_2 system obtained by additive manufacturing (specifically, direct laser deposition). The properties of the composites obtained were investigated at high temperatures (up to 1000 °C). The feasibility of the fabrication of a composite nanostructure of alloy with advanced physicomechanical properties was shown. The introduction of reinforcing TiB_2 particles into an Inconel 625 matrix was confirmed to increase the microhardness and tensile strength of the material obtained. Apparently, the composite structure of the samples facilitates the realisation of several strengthening mechanisms: (1) a grain boundary mechanism that causes strengthening and dislocation movement; (2) a mechanism based on the grain structure breakdown and Hall–Petch relationship realisation.

Keywords: metal-matrix composites; structure; properties; phase composition

Citation: Promakhov, V.; Matveev, A.; Klimova-Korsmik, O.; Schulz, N.; Bakhmat, V.; Babaev, A.; Vorozhtsov, A. Structure and Properties of Metal-Matrix Composites Based on an Inconel 625–TiB_2 System Fabricated by Additive Manufacturing. *Metals* **2022**, *12*, 525. https://doi.org/10.3390/met12030525

Academic Editor: Antonio Riveiro

Received: 16 February 2022
Accepted: 18 March 2022
Published: 21 March 2022

1. Introduction

Thanks to their mechanical properties, Inconel alloys have a good record as functional materials used at high temperatures in chemically aggressive environments and under high loads [1]. The development of additive manufacturing technologies has revealed the potential of these alloys as powder raw stock (initial powders for the production of materials) for additive manufacturing machines) [2–4]. It should be noted that the use of additive manufacturing technologies (AM) saves time, costs and reduces the role of the human factor in the manufacturing process compared to traditional sintering and casting technologies. Therefore, in sintering and casting technology, the preliminary stages of design and manufacture of mould and injection mould would not be necessary. It also removes some of the limitations on the shape of items manufactured [5]. According to a series of research works, a combination of advantages of AM and advanced mechanical properties of Inconel alloys makes it possible to cost-effectively obtain products with complex geometry that can be used in aggressive conditions (high temperatures, high mechanical stress, elevated oxidizing conditions, etc.). Examples include turbines and engine injectors, communication units, etc., where longer service life is ensured while reducing overall weight and production costs [6–10]. Research work [11] aimed to optimize 3D printing modes for high-temperature items made of a nickel-based alloy. The authors also investigated the mechanical properties of experimental samples and compared thermal treatment modes. Powders with spherical particles made of a high-temperature nickel-based alloy identical to Inconel 718 were used as raw stock. The samples were fabricated using an SLM 280HL printing system (IPG Laser). An optimal SLM printer mode was set: laser power at 190 ± 20 W and laser scanning speed at 855 ± 90 mm/s. With these parameters, a material with a homogeneous structure and a minimum pore ratio (2.5%) was obtained. Moreover, the authors established that the tensile strength of the fabricated

materials was 1070 MPa. It exceeds that of the materials obtained using conventional manufacturing techniques by 118 MPa.

Though high values of the physicomechanical properties of the materials fabricated from Inconel alloys were achieved, the aerospace, engine manufacturing and automotive industries demand still higher operating temperatures for engines and power generation units to improve their energy performance and overall performance [12]. The demand rises for such higher-level parameters as durability, strength, wear resistance, operability at high temperatures, resistance to multi-cycle loading, cracking resistance, etc. Classical condensed-state physics dictate that material properties are determined by their structure; hence, changes in the structure may provide new (sometimes unique) properties. Therefore, the creation of a new type of Inconel-based powder composition type, combined with the development of additive manufacturing technologies, can make a significant contribution to an increase in the energy performance of the fabricated items. Metal-matrix composites with ceramic inclusions can provide advanced physicomechanical properties. Metal-matrix composites comprise a metal or intermetallic matrix wherein ceramic inclusions are evenly distributed [13,14]. These composites have higher mechanical strength, durability, wear resistance and operating temperatures, and those values cannot be achieved for conventional metallic alloys [15–18]. Metal-matrix composites are normally obtained from a mixture of Inconel powders and ceramic powders: TiC [19], WC [20] and CrC [21]. This technique produces composites that comprise a metal-matrix wherein reinforcing ceramic particles are distributed. However, with this technique, the wettability of ceramic inclusions is reduced, and this leads to their agglomeration and creation of an inhomogeneous structure while also reducing the samples' density and creating a large amount of pores. To improve the structure homogeneity and density, the laser beam power needs to be increased, which also increases the wettability and reflow of the ceramic particles. However, increased power results in additional energy consumption and complexity of the laser deposition workflow [22].

In Ref. [23] the authors have demonstrated that reducing the size of the ceramic particles of titanium carbide powder (TiC) and using mechanical activation has enabled them to achieve homogeneous distribution of ceramic particles on the surface of Inconel alloy particles in the initial powder mixture. The use of this technique has allowed to achieve a homogeneous composite structure after additive deposition while also reducing the amount of pores in the samples. However, even with these results, the authors had to find additive deposition modes by trial and error and feed more laser power per unit of length (LEIPUL) to achieve the required physicomechanical properties. It was shown that, for LEIPUL at 72–100 kJ/m, the tensile strength of the fabricated composites was 1077.3 MPa, the yield stress was 659.3 MPa and the elongation was 20.7%.

From the above, the problem of increasing the wettability of ceramic inclusions without additional treatment stages and increasing laser beam power arises. One of the possible ways to solve this problem is the creation of composite powders for laser deposition systems. Particles of such powders consist of metal-matrixes with evenly distributed ceramic inclusions. The use of these powders in additive manufacturing would allow for increased wettability of ceramic particles with matrix metal melt. In this case, each ceramic particle is coated with a layer of molten matrix material. The layer between the ceramic particles prevents their recrystallization and agglomeration processes. This, in turn, leads to a more uniform distribution of the majority of isolated particles. This allows increasing material density without additional treatment or extra power input into the laser beam.

In our previous works [24,25], we obtained composite powder materials, CrNi–TiN and (Ni–Ti)–TiB_2, from CrN–TiNi and NiB–Ti powder mixtures using self-propagating high-temperature synthesis (SHS). The structure of these powders consisted of a CrNi/Ni-Ti intermetallic matrix wherein TiN/TiB_2 particles were evenly distributed. The composite structure was formed in situ and the formation process was supported by exothermic reactions between the initial mixture components. It should be noted that the SHS process is maintained by the heat from these reactions and, therefore, no additional energy input

is needed [26]. The obtained composite powders were used as raw stock in additive deposition systems. In research work [27], it was shown that the structure of the materials obtained by direct laser deposition inherits the structure of the particles of the SHS powders. Titanium nitride particles are evenly distributed in the intermetallic CrNi matrix. The sizes of ceramic particles ranged between 0.3 and 9 µm, whereas the average size was 2.8 µm. The average microhardness (under load 500 g) was 760 HV. The research findings have demonstrated the successful use of composite metal-matrix powders as a raw stock for additive deposition systems. However, in the research [28], it was found that the presence of large amounts of the ceramic phase in the materials (50–90 wt%) fabricated by AM using composite NiTi–TiB_2 powders leads to the emergence of considerable internal stresses, which facilitates crack formation, resulting in brittle destruction. Here, the authors suggested that the use of composite SHS powders as additives to Inconel 625 powders in the amount of 5 wt% will result in a more uniform distribution of the ceramic particles in the metal-matrix while reducing the impact of internal stresses and realising multiple reinforcement mechanisms, specifically dislocation-based and dispersion-based ones [29].

Thus, the purpose of this research is the investigation of the structure and mechanical properties of the materials of 95 wt% Inconel 625 + 5 wt% NiTi+TiB_2 where the materials had been obtained by direct laser deposition.

2. Materials and Methods

2.1. Initial Materials

Inconel 625 (Hoganas) powders and a composite NiTi–TiB_2 metal-matrix powder were used as the initial components of the mixture for fabricating samples by direct laser deposition. It was shown that the sphericity of the Hoganas powder was 0.805. On the surface of the powders, there are individual satellites with a shape that is close to a polyhedron (Figure 1a). The sizes of the powder particles ranged between 40 and 180 µm, whereas the average size was 90 µm (Figure 1b). The chemical composition of the Inconel 625 powder is presented in Table 1.

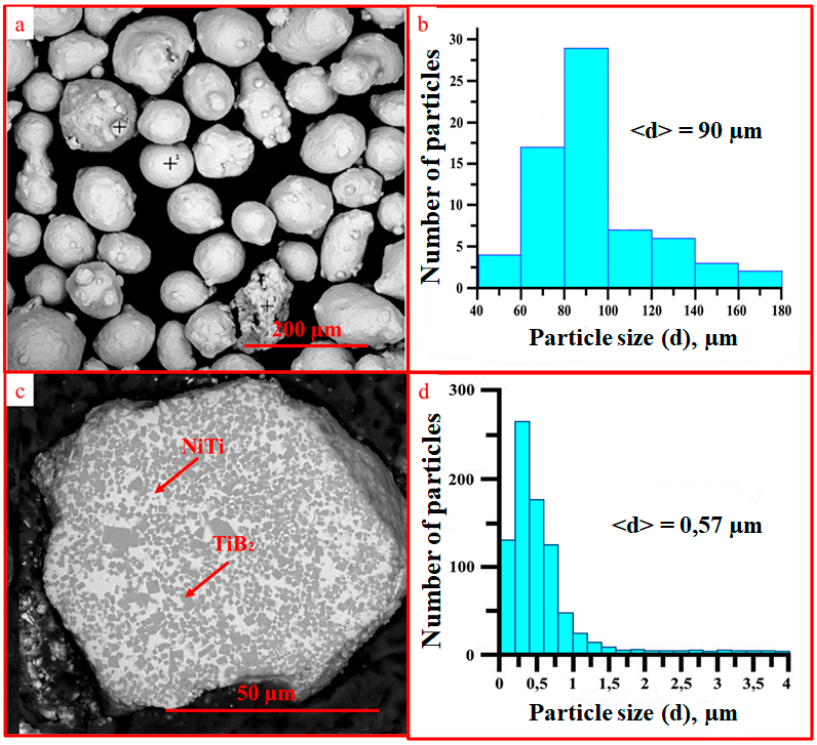

Figure 1. SEM image of Inconel 625 powder particles and histogram of their distribution by size (**a**,**b**); SEM image of the structure of NiTi–TiB_2 composite powder particles and histogram of TiB_2 particle size distribution in the NiTi matrix (**c**,**d**).

Table 1. Chemical composition of the Inconel 625 powder.

Manufacturer	Chemical Composition of the Powder								
	Ni	**Cr**	**Fe**	**Mo**	**P**	**Nb**	**B**	**Ti**	**Other**
Inconel 625 (Hoganas)	Main	20.8	0.51	8.9	-	3.51	-	-	0.08
	Si	**Co**	**C**	**Mn**	**Al**	**O_2**	**S**	**Cu**	
	0.43	-	0.01	0.37	0.01	0.07	-	-	

The NiTi–TiB_2 powder was obtained by self-propagating high-temperature synthesis from the NiB–Ti powder mixture using the methodology presented in the article [25]. The cakes obtained in the process of SHS were crushed into powder with the particle size distribution of 50–150 µm. The structure of powder particles is represented by an intermetallic NiTi matrix wherein TiB_2 particles are distributed (Figure 1c). The average size of ceramic particles in the metal-matrix was 0.5 µm, and the largest contribution to the distribution was made by particles with the size ranging from 0.1 to 0.2 µm.

The Inconel 625 and NiTi–TiB_2 powders were mixed in the following ratio: 95 wt% Inconel 625 + 5 wt% NiTi–TiB_2. The mixing was carried out in a ball mill for 30 min at a rotation speed of 14 Hz.

2.2. Process of Obtaining Materials by Direct Laser Deposition from a Powder Mixture of 95 wt% Inconel 625 + 5 wt% NiTi–TiB_2

The samples were obtained by direct laser deposition of the powder mixture on a substrate made of 7 mm thick RCE36 steel. For weld deposition, an LS-3 ytterbium fibre laser manufactured by IRE-Polyus (LLC NTO "IRE-Polyus", Fryazino, Moscow region, Russia) was used (Figure 2a). Concurrent dual-side deposition was chosen as the deposition strategy (Figure 2b). It should be noted that such a deposition strategy makes it possible to avoid defects associated with the distortion of the shape of the materials obtained.

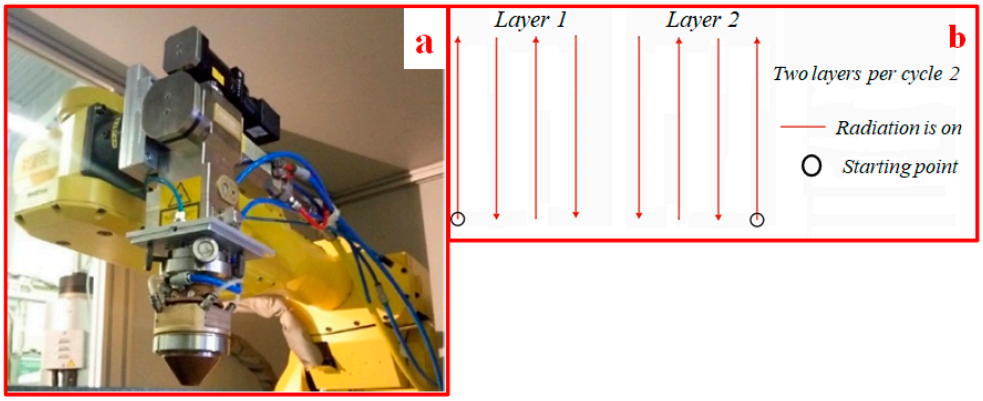

Figure 2. Ytterbium fibre laser LS-3 (**a**); concurrent dual-side deposition strategy (**b**).

Laser radiation was focused using an FLW D30 process head by IPG Photonics (IPG Photonics Corp. Oxford, MA, USA). A COAX9 coaxial weld deposition nozzle manufactured by Fraunhofer ILT (Fraunhofer ILT, Aachen, Germany) was used to form a gas-powder jet. An LRM-200iD_7L industrial robot by Fanuc (Fanuc Co., Ltd., Osino, Japan) was used as a manipulator. The parameters of the laser deposition mode are presented in Table 2.

2.3. Research Methods

The phase composition of the materials obtained from the powder mixture with 95 wt% Inconel 625 + 5 wt% NiTi+TiB_2 by direct laser deposition was investigated on a Shimadzu XRD-6000 diffractometer (on Cuka radiation and Ni filter) (by Shimadzu Corporation, Tokyo, Japan). The phases were determined by comparing the peaks and the obtained

diffraction patterns against the Powder Diffraction File 4 database of the International Center for Diffraction Data (ICDD®; Newtown Square, PA, USA). The structure of the materials was investigated using optical and scanning electron metallography on a T-Scan microscope. The hardness was measured on a Buehler Wilson Micromet 6040 (Buehler LLC, Lake Bluff, IL, USA) hardness tester with a Thixomet Pro image analyser (Nikon Corp., Tokyo, Japan). The tensile tests were carried out on an Instron universal static testing system (Illinois Tool Works Inc., Glenview, IL, USA).

Table 2. Direct laser growth parameters.

Beam Diameter in the Treatment Area, mm	Power, W	Side Beads Deposition Rate, mm/s	Intermediate Beads Deposition Rate, mm/s	Powder Consumption, g/min	X Offset, mm	Z Offset, mm
1.5	500	10	15	5.1	0.7	0.2

3. Results and Discussion

3.1. Phase Composition and Structure of the Materials 95 wt% Inconel 625 + 5 wt% NiTi–TiB_2

Figure 3a shows the appearance of the materials obtained by direct laser deposition from a powder mixture of 95 wt% Inconel 625 + 5 wt% NiTi–TiB_2. The use of the concurrent dual-side deposition strategy has made it possible to obtain rectangular materials with a uniform structure of shell layers and without significant defects. An X-ray pattern of the materials and an SEM image of their structure are shown in Figure 3b–d, and the results of the X-ray diffraction analysis are presented in Table 3. During laser deposition, a composite metal-matrix structure is formed in the materials. In a nickel-based matrix (Inconel 625), rectangular and spherical titanium diboride particles are evenly distributed. The sizes of the ceramic particles ranged between 0.05 and 1.2 µm, whereas the average size was 0.22 µm (Figure 1b). Here, the largest contribution to the particle size distribution was made by particles whose size varies in the range from 0.1 to 0.2 µm. It should be noted that the structure of the obtained materials is similar to the structure of the NiTi–TiB_2 SHS composites obtained in Ref. [25]. At the same time, titanium diboride particles in SHS composites have either an irregular angular or rectangular shape. Presumably, some TiB_2 particles melt during laser deposition, which changes their shape towards a spherical one.

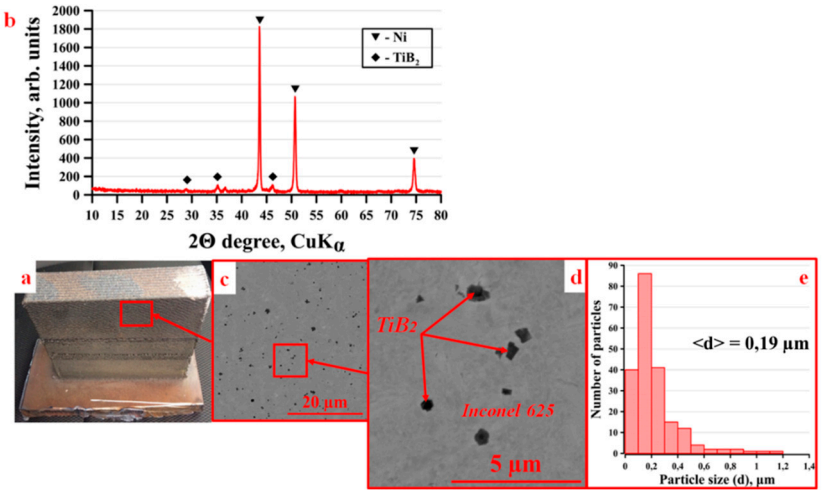

Figure 3. **(a)** Appearance of the materials obtained by selective laser deposition from a powder mixture consisting of 95 wt% Inconel 625 + 5 wt% NiTi–TiB_2; (**b**) X-ray pattern of the obtained materials; (**c**,**d**) SEM images of the structure of the materials; (**e**) size distribution of TiB_2 particles in these materials.

Table 3. Results of the X-ray diffraction analysis of the materials obtained by selective laser deposition from a powder mixture of 95 wt% Inconel 625 + 5 wt% NiTi–TiB_2.

Discover Phases	Phase Content, Mass%	Lattice Parameters, Å
Ni	95	a = 3.6218
TiB_2	<5	a = 2.9468 c = 3.1359

3.2. Mechanical Properties of the Material 95 wt% Inconel 625 + 5 wt% NiTi–TiB_2

It is known that uneven distribution of ceramic particles in a metal-matrix and the presence of large particles and agglomerates lead to high fluctuations of microhardness in the composite [30]. Thus, it is necessary to measure the microhardness in the investigated samples both along the deposition direction and across it in order to compare the resulting values for different layers of the sample.

The hardness of the materials obtained by direct laser deposition from a powder mixture of 95 wt% Inconel 625 + 5 wt% NiTi–TiB_2 was measured from a cut made from the upper surface of the sample across the deposition direction (Figure 4a,b). The measurement results are provided in Figure 4c.

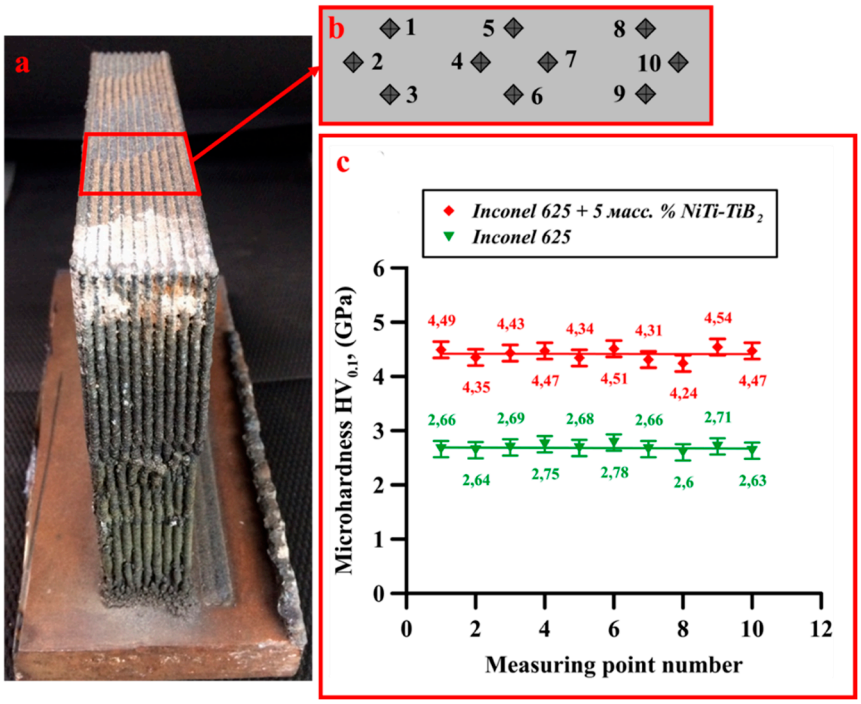

Figure 4. (a) Appearance of the materials obtained by direct laser deposition from a powder mixture of 95 wt% Inconel 625 + 5 wt% NiTi–TiB_2; (**b**) a schematic of the distribution of indenter marks on the sample; (**c**) a diagram of the distribution of hardness values in the sample.

The microhardness of the materials varied from 4.24 to 4.54 GPa, and the average value of microhardness was 4.42 ± 0.1 GPa. It was found that the distribution of microhardness throughout the sample was linear. There was no significant deviation of microhardness between the layers of the deposited material. For the sake of comparison, the microhardness of the materials obtained by selective laser deposition from pure Inconel 625 has been measured. It was found that the microhardness of the samples varied from 2.6 to 2.84 GPa, and the average microhardness was 2.73 ± 0.1 Gpa. The distribution was linear as well. Therefore, the addition of a composite metal-matrix NiTi–TiB_2 SHS powder to Inconel 625 powder in the amount of 5 wt% led to an increase in the microhardness of the material by 1.5 times as compared to the materials obtained from pure Inconel 625, and the uniform

distribution of titanium diboride particles in the sample and their size (0.19 μm) allow for maintaining the uniformity of microhardness throughout the material.

Figure 5 shows a diagram of specimens for stress testing and a stress–strain diagram with a tensile test of the samples fabricated by the deposition of a 95 wt% Inconel 625 + 5 wt% NiTi–TiB_2 powder mixture and samples deposited from pure Inconel 625. The results of the tests are presented in Table 4.

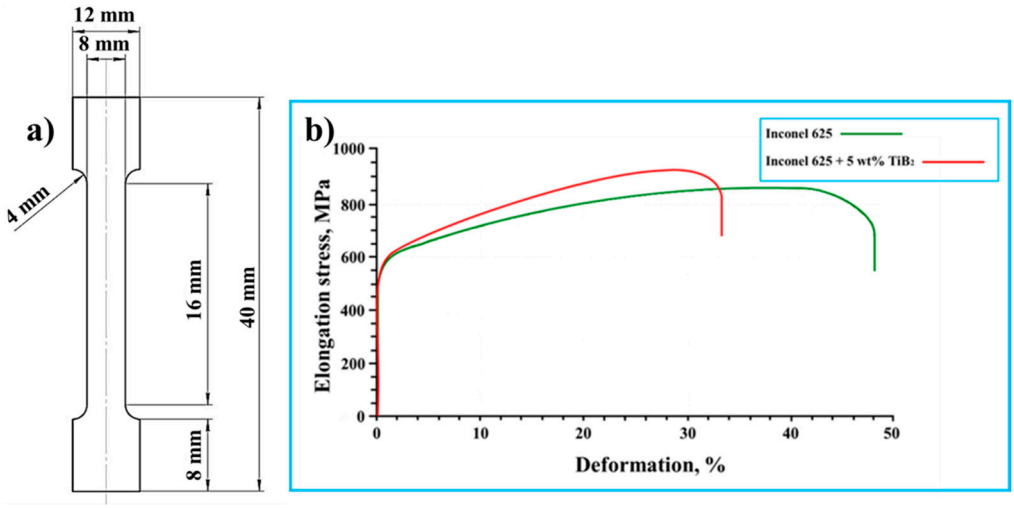

Figure 5. (**a**) Diagram of specimens for stress testing; (**b**) stress–strain diagram obtained during tensile testing of samples obtained by the deposition of a powder mixture of 95 wt% Inconel 625 + 5 wt% NiTi–TiB_2 powder mixture, as well as from testing the samples deposited from pure Inconel 625.

Table 4. Tensile test results for materials produced by selective laser deposition.

Initial Mixture Composition	Elastic Modulus (E), MPa	Relative Elongation (%)	Tensile Strength (σ_B), MPa
Inconel 625 + 5 wt% NiTi–TiB_2	550	33	920
Inconel 625	545	48	850

The addition of the 5 wt% NiTi–TiB_2 powder resulted in a slight increase in the elastic modulus as compared to the materials made from pure Inconel 625 powder. In this case, an increase in the tensile strength from 850 to 920 MPa is observed, which is accompanied by a decrease in the plasticity of the material.

Figure 6 shows the appearance of the three-point bend test setup and a schematic of the shape and dimensions of the Inconel 625 and 95 wt% Inconel 625 + 5 wt% NiTi–TiB_2 samples, as well as the dependencies of the bending strength and bending deformation rate of the samples after three-point bending tests both at room and at elevated temperatures. It has been established that, at room temperature, the bending strength and bending deformation rate of the materials obtained from pure Inconel 625 were 2095 MPa and 5.8%, respectively. An increase in the temperature to 1000 °C caused the mechanical parameters to decrease to 687 MPa and 0.7%, respectively. The addition of the 5 wt% of the NiTi–TiB_2 composite powder led to an increase in the ultimate strength both at room temperature (2410 MPa) and at elevated temperatures (760 MPa at 1000 °C). Meanwhile, the addition of composite particles led to a decrease in the relative bending deformation rate of the material both at room and at elevated temperatures.

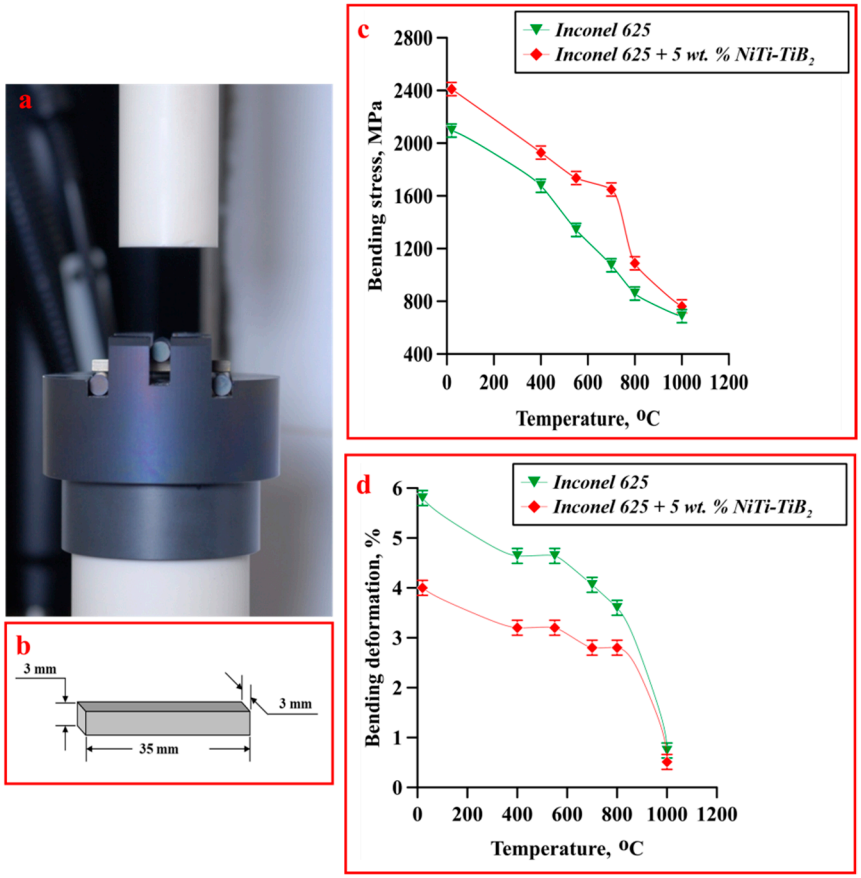

Figure 6. (**a**) Appearance of the three-point bending tester; (**b**) a schematic representation of the shape and dimensions of the 95 wt% Inconel 625 + 5 wt% NiTi–TiB_2 sample; dependencies of bending strength and bending deformation rate of samples after three-point bending tests conducted at room (**c**) and at elevated (**d**) temperatures.

An increase in the microhardness of the samples obtained from a powder mixture of 95 wt% Inconel 625 + 5 wt% NiTi–TiB_2 and their bending strength at three-point bending tests are associated with a number of factors. Firstly, high hardness of titanium diboride (hardness: 25–35 GPa) integrally contributes to the increase in the hardness of the materials obtained. Secondly, in the course of laser deposition, titanium diboride nanoparticles act as nuclei during crystallization, which can reduce the average grain size and increase strength [31]. Thus, the composite structure of the samples facilitates the realisation of several strengthening mechanisms: (1) a grain boundary mechanism that causes strengthening and dislocation movement; (2) a mechanism based on the grain structure breakdown and Hall–Petch relationship [32] realisation.

4. Conclusions

The present research has shown that the use of powders that are composite in nature and have been obtained by self-propagating high-temperature synthesis increases the wettability of the ceramic particles with matrix metal. This, in turn, improves the quality of the particle–matrix boundary while reducing the porosity and increasing the uniformity of the particles' distribution in the matrix. The structure of the fabricated materials is represented by the Inconel 625 matrix alloy and TiB_2 ceramic inclusions. The average size of the ceramic particles did not exceed 200 nm. It was shown that adding 5 wt% of a NiTi–TiB_2 composite metal-matrix SHS powder to Inconel 625 powder increased the microhardness of the resulting material by 1.5 times as compared to the materials obtained from pure Inconel 625. Here, increased tensile strength and bending strength are observed in the course of tensile tests and bending tests, respectively, and the plasticity is decreased

by 15% as compared to the samples from pure Inconel 625. Apparently, the composite structure of the samples facilitates the realisation of several strengthening mechanisms: (1) a grain boundary mechanism that causes strengthening and dislocation movement; (2) a mechanism based on the grain structure breakdown and Hall–Petch relationship realisation.

Author Contributions: Conceptualization, V.P. and A.M.; methodology, V.P. and O.K.-K.; formal analysis, A.V.; writing—original draft preparation, N.S., O.K.-K., A.B. and A.M.; writing—review and editing, A.M., A.B. and V.P.; visualization, V.B.; supervision, A.V.; project administration, V.P. All authors have read and agreed to the published version of the manuscript.

Funding: This research was funded by the Russian Science Foundation, grant number 20-79-10086.

Institutional Review Board Statement: Not applicable.

Informed Consent Statement: Not applicable.

Data Availability Statement: Not applicable.

Conflicts of Interest: The authors declare no conflict of interest.

References

1. Fox, G.R.; Liang, H. Wear Mode Comparison of High-Performance Inconel Alloys. *J. Tribol.* **2010**, *132*, 021603. [CrossRef]
2. Pleass, C.; Jothi, S. Influence of powder characteristics and additive manufacturing process parameters on the microstructure and mechanical behaviour of Inconel 625 fabricated by Selective Laser Melting. *Addit. Manuf.* **2018**, *24*, 419–431. [CrossRef]
3. Dhinakaran, V.; Fathima Yasin Fahmidha, A.; Jagadeesha, T.; Sathish, T.; Stalin, B. Wire Arc Additive Manufacturing (WAAM) process of nickel based superalloys—A review. *Mater. Today Proc.* **2020**, *21*, 920–925. [CrossRef]
4. Kappes, B.; Moorthy, S.; Drake, D.; Geerlings, H.; Stebner, A. Machine Learning to Optimize Additive Manufacturing Parameters for Laser Powder Bed Fusion of Inconel 718. In Proceedings of the 9th International Symposium on Superalloy 718 & Derivatives: Energy, Aerospace, and Industrial Applications, Pittsburgh, PA, USA, 13 May 2018.
5. Wong, K.V.; Hernandez, A. A review of additive manufacturing. *Int. Sch. Res. Not.* **2012**, *2012*, 208760. [CrossRef]
6. Anush Raj, B.; Winowlin Jappes, J.T.; Adam Khan, M.; Dillibabu, V.; Brintha, N.C. Direct metal laser sintered (DMLS) process to develop Inconel 718 alloy for turbine engine components. *Optik* **2020**, *202*, 163735. [CrossRef]
7. Schilke, P.W.; Foster, A.D.; Pepe, J.J. *Advanced Gas Turbine Materials and Coatings*; General Electric Company: New York, NY, USA, 1991.
8. Sharma, P.; Chakradhar, D.; Nerendranath, S. Evaluation of WEDM performance characteristics of Inconel 706 for turbine disk application. *Mater. Des.* **2015**, *202*, 163735. [CrossRef]
9. Farid, A.A.; Sharif, S.; Namazi, H. Effect of machining parameters and cutting edge geometry on surface integrity when drilling and hole making in Inconel 718. *SAE Int. J. Mater. Manuf.* **2009**, *2*, 564–569. [CrossRef]
10. Kianian, B. *Wohlers Report 2017: 3D Printing and Additive Manufacturing State of the Industry, Annual Worldwide Progress Report: Chapters Titles: The Middle East, and Other Countries*, 22nd ed.; Wohlers Associates: Fort Collins, CO, USA, 2017.
11. Mazalov, A.; Shmatov, D.; Zelenina, L.; Platko, D.; Promakhov, V.; Vorozhtsov, A.; Schulz, N. Researching the Properties of Samples Fabricated Using Selective Laser Melting from A High-Temperature Nickel-Based Alloy. *Appl. Sci.* **2021**, *11*, 1419. [CrossRef]
12. Rao, H.; Oleksak, R.P.; Favara, K.; Harooni, K.; Dutta, B.; Maurice, D. Behavior of yttria-stabilized zirconia (YSZ) during laser direct energy deposition of an Inconel 625-YSZ cermet. *Addit. Manuf.* **2020**, *31*, 100932. [CrossRef]
13. Zhukov, I.A.; Kozulin, A.A.; Khrustalyov, A.P.; Matveev, A.E.; Platov, V.V.; Vorozhtsov, A.B.; Zhukova, T.V.; Promakhov, V.V. The impact of particle reinforcement with Al_2O_3, TiB_2, and TiC and severe plastic deformation treatment on the combination of strength and electrical conductivity of pure aluminum. *Metals* **2019**, *9*, 65. [CrossRef]
14. Matveev, A.; Zhulov, I.; Ziatdinov, M.; Zhukov, A. Planetary milling and self-propagating high-temperature synthesis of Al-TiB_2 composites. *Materials* **2020**, *13*, 1050. [CrossRef] [PubMed]
15. Hashim, J.; Looney, L.; Hashmi, M.S. Metal matrix composites: Production by the stir casting method. *J. Mater. Process. Technol.* **1999**, *92*, 1–7. [CrossRef]
16. Tjong, S.C. Novel nanoparticle-reinforced metal matrix composites with enhanced mechanical properties. *Adv. Eng. Mater.* **2007**, *9*, 639–652. [CrossRef]
17. Vorozhtsov, S.A.; Eskin, D.G.; Tamayo, J.; Vorozhtsov, A.B.; Promakhov, V.V.; Averin, A.A.; Khrustalyov, A.P. The application of external fields to the manufacturing of novel dense composite master alloys and aluminum-based nanocomposites. *Metall. Mater. Trans. A* **2015**, *46*, 2870–2875. [CrossRef]
18. Rawal, S.P. Metal-matrix composites for space applications. *JOM* **2001**, *53*, 14–17. [CrossRef]
19. Wilson, J.M.; Shin, Y.C. Microstructure and wear properties of laser-deposited functionally graded Inconel 690 reinforced with TiC. *Surf. Coat. Technol.* **2012**, *207*, 517–522. [CrossRef]

20. Liu, Z.; Cabrero, J.; Niang, S.; Al-Taha, Z.Y. Improving corrosion and wear performance of HVOF-sprayed Inconel 625 and WC-Inconel 625 coatings by high power diode laser treatments. *Surf. Coat. Technol.* **2007**, *201*, 7149–7158. [CrossRef]
21. Nurminen, J.; Näkki, J.; Vuoristo, P. Microstructure and properties of hard and wear resistant MMC coatings deposited by laser cladding. *Int. J. Refract. Met. Hard Mater.* **2009**, *27*, 472–478. [CrossRef]
22. Gu, D.; Hong, C.; Dai, D.; Gasser, A.; Weisheit, A.; Kelbassa, I.; Zhong, M.; Poprawe, R. Combined strengthening of multi-phase and graded interface in laser additive manufactured TiC/Inconel 718 composites. *J. Phys. D Appl. Phys.* **2013**, *47*, 045309. [CrossRef]
23. Hong, C.; Gu, D.; Dai, D.; Alkhayat, M.; Urban, W.; Yuan, W.; Cao, S.; Gasser, A.; Weisheit, A.; Kelbassa, I.; et al. Influence of scan strategy and process parameters on microstructure and its optimization in additively manufactured nickel alloy 625 via laser powder bed fusion. *Mater. Sci. Eng. A* **2015**, *635*, 118–128. [CrossRef]
24. Matveev, A.; Promakhov, V.; Schulz, N.; Vorozhtsov, A. Synthesis of Metal Matrix Composites Based on CrxNiy-TiN for Additive Technology. *Materials* **2021**, *14*, 5914. [CrossRef] [PubMed]
25. Promakhov, V.; Matveev, A.; Schulz, N.; Grigoriev, M.; Olisov, A.; Vorozhtsov, A.; Zhukov, A.; Klimenko, V. High-Temperature Synthesis of Metal–Matrix Composites (Ni-Ti)-TiB_2. *Appl. Sci.* **2021**, *11*, 2426. [CrossRef]
26. Amosov, A.P.; Makarenko, A.G.; Samboruk, A.R.; Seplyarskii, B.S.; Samboruk, A.A.; Gerasimov, I.O.; Orlov, A.V.; Yatsenko, V.V. Granulation in the powder technology of self-propagating high-temperature synthesis. *Russ. J. Non-Ferr. Met.* **2013**, *54*, 267–273. [CrossRef]
27. Artyukhova, N.; Anikeev, S.; Promakhov, V.; Korobenkov, M. The Effect of Cobalt on the Deformation Behaviour of a Porous TiNi-Based Alloy Obtained by Sintering. *Materials* **2021**, *14*, 7584. [CrossRef]
28. Promakhov, V.; Zhukov, A.; Ziatdinov, M.; Zhukov, I.; Schulz, N.; Kovalchuk, S.; Dubkova, Y.; Korsmik, R.; Klimova-Korsmok, O.; Turichin, D.; et al. Inconel 625/TiB_2 metal matrix composites by direct laser deposition. *Metals* **2021**, *9*, 141. [CrossRef]
29. Lorusso, M.; Aversa, A.; Manfredi, D.; Calignano, F.; Ambrosio, E.P.; Ugues, D.; Pavese, M. Tribological behavior of aluminum alloy AlSi10Mg-TiB_2 composites produced by direct metal laser sintering (DMLS). *J. Mater. Eng. Perform.* **2016**, *25*, 3152–3190. [CrossRef]
30. Zhou, S.; Xu, T.; Hu, C.; Wu, H.; Liu, H.; Ma, X. Utilizing carbon nanotubes in ceramic particle reinforced MMC coatings deposited by laser cladding with Inconel 625 wire. *J. Mater. Res. Technol.* **2021**, *13*, 2026–2042. [CrossRef]
31. Li, W.; Yang, Y.; Liu, J.; Zhuo, Y.; Li, M.; Wen, S.; Wei, Q.; Yan, C.; Shi, Y. Enhanced nanohardness and new insights into texture evolution and phase transformation of TiAl/TiB_2 in-situ metal matrix composites prepared via selective laser melting. *Acta Mater.* **2017**, *136*, 90–104. [CrossRef]
32. Chen, L.; Sun, Y.; Li, L.; Ren, Y.; Ren, X. In situ TiC/Inconel 625 nanocomposites fabricated by selective laser melting: Densification behavior, microstructure evolution, and wear properties. *Appl. Surf. Sci.* **2020**, *518*, 145981. [CrossRef]